

THEORY OF DECOUPLING IN THE MIXED PHASE OF EXTREMELY TYPE-II LAYERED SUPERCONDUCTORS

J. P. Rodriguez

Dept. of Physics and Astronomy, California State University, Los Angeles, CA 90032.

Abstract

The mixed phase of extremely type-II layered superconductors in perpendicular magnetic field is studied theoretically via the layered XY model with uniform frustration. A partial duality analysis is carried out in the weak-coupling limit. It consistently accounts for both intra-layer (pancake) and inter-layer (Josephson) vortex excitations. The main conclusion reached is that dislocations of the two-dimensional (2D) vortex lattices within layers drive a unique second-order melting transition at high perpendicular fields between a low-temperature superconducting phase that displays a Josephson effect and a high-temperature “normal” phase that displays no Josephson effect. The former state is best described by weakly coupled 2D vortex lattices, while the latter state is best characterized by a decoupled vortex liquid. It is further argued on the basis of the duality analysis that the second-order melting transition converts itself into a first-order one as the perpendicular field is lowered and approaches the dimensional cross-over scale. The resulting critical endpoint potentially accounts for the same phenomenon that is observed in the mixed phase of clean high-temperature superconductors.

PACS Indices: 74.60.-w, 74.25.Dw, 74.25.Ha, 74.60.Ge

I. Introduction

The nature of the thermodynamic phase diagram in clean high-temperature superconductors in external magnetic field has been elucidated only recently.¹ Experimental evidence for a first-order melting transition of the Abrikosov vortex lattice has been obtained from the measurement of a jump in the magnetization and from the measurement of a latent heat.^{2,3} These two quantities are found to satisfy the Clausius-Clapeyron relation, which indicates that the first-order transition is indeed thermodynamic. Although the existence of such a melting transition was expected on theoretical grounds due to the extreme type-II and anisotropic character of high-temperature superconductors,⁴ the multi-critical phenomenon exhibited by the associated phase diagram for the mixed phase was not. In particular, the first-order melting line begins at (or near) the zero-field transition, but it ends strangely in the middle of the field versus temperature ($T - H_{\perp}$) plane. The critical end point, furthermore, coincides (or is near) a multi-critical point, from which a nearly field-independent “vertical” depinning line of the vortex lattice begins at higher fields.^{5,6} A weakly temperature-dependent “horizontal” second-peak line also continues on from the multi-critical point to lower temperatures. Bulk pinning becomes appreciably stronger at fields above this line.⁷

The first-order melting observed in clean high-temperature superconductors is commonly interpreted theoretically in terms of elastic medium descriptions of the vortex lattice.⁴ The melting point in such theories is usually determined by the Lindemann criterion, however, which cannot predict the nature of the transition. In other words, the theory is compatible with either a first-order, a second-order, or even a cross-over transition. Elastic medium theory has also been used to describe the mixed phase of layered superconductors in particular.⁸ A first-order decoupling transition is predicted to occur in the extreme type-II limit, beyond which absolutely no Josephson coupling remains in between the layers.⁹ A subsequent high-temperature analysis of the anisotropic XY model with uniform frustration has demonstrated, however, that a small degree of local Josephson coupling must survive the decoupling transition.^{10,11} Last, it is important to remark that most elastic medium calculations to date have been performed in the gaussian approximation.⁴ They therefore neglect important topological excitations of the vortex lattice, such as dislocations, that can drive the melting transition.^{12,13}

Other more numerical approaches to the theoretical description of the mixed phase in clean high-temperature superconductors have succeeded in obtaining a clear first-order melting transition. These include Monte-Carlo simulations of both the frustrated XY model^{14,15} and of Ginzburg-Landau theory.¹⁶ The former simulations are plagued, however, by equilibration problems at low temperatures due to the artificial pinning caused by the underlying XY model lattice.¹¹ The latter simulations of Ginzburg-Landau theory, on the other hand, are performed in the lowest-Landau-level approximation. This approximation is in principle valid only in the vicinity of the mean-field H_{c2} transition, which remains far from the vortex-lattice melting line observed experimentally in high-temperature superconductors because of anisotropy.^{2,3}

In this paper, we shall develop a theory for decoupling in the mixed phase of extreme type-II layered superconductors that is based on an analysis of the corresponding layered XY model with uniform frustration. The analysis is effected through a *partial* duality transformation that leads to a useful neutral Coulomb-gas (CG) description for the Josephson coupling.^{17–20} Unlike some of the Coulomb-gas analyzes of the layered XY model that have been performed in the past,^{21–24} both gaussian and topological excitations of the vortex lattice within layers are *consistently* accounted for in this approach. This consistency is responsible for the primary result of the paper, which is that there exists a unique second-order transition in the weak-coupling limit that separates a coupled superconducting phase at low temperature from a decoupled “normal” state at high temperature. In the context of the mixed phase, the weak-coupling limit is reached at field components perpendicular to the layers that are large compared to the dimensional cross-over scale $B_{\perp}^* = \Phi_0/\Lambda_0^2$ (see Fig. 1). Here, Λ_0 denotes the Josephson penetration length. Note that the criterion used throughout to discriminate between a coupled and a decoupled state is the presence or absence of a macroscopic Josephson effect, respectively. The above result implies that neither the Friedel scenario,^{4,25} which is a state composed of decoupled superconducting layers, nor a “line-liquid” state,^{14,24,26} which we define here as a set of normal layers in external magnetic field that exhibit a Josephson effect, are likely to be thermodynamic states in the mixed phase of extreme type-II layered superconductors when disorder is absent. The prediction of a unique phase transition in the uniformly frustrated XY model with anisotropy is notably consistent with recent extensive Monte

Carlo simulations.¹⁵ It was also anticipated by various authors in studies of the layered XY model without perpendicular frustration.^{21,22,27,28}

The duality analysis mentioned above is also employed in the paper to map out the phase diagram of the layered XY model with uniform frustration. A finite number of layers is assumed. The weak-coupling limit at high perpendicular fields is found to contain a low-temperature phase made up of independent two-dimensional (2D) vortex lattices that sustain a Josephson effect. This phase is separated from a decoupled liquid of planar vortices at high temperatures by a second-order melting transition akin to that shown by an isolated 2D vortex lattice.^{29–33} The existence of such a second-order melting transition is demonstrated by making note of a formal equivalence between the Coulomb gas descriptions of the layered XY model with and without frustration.^{20,34} Also, the former smectic 2D vortex-lattice phase is likely to be a type of “supersolid” matter (see sect. IV.C and ref. 13). The above weak-coupling analysis is then shown to break down at sufficiently low perpendicular fields of order the dimensional cross-over scale B_{\perp}^* . It is argued that this breakdown signals a cross-over transition to a flux-line lattice regime at low fields and temperatures, while that it signals a first-order decoupling transition to a potentially defective flux-line lattice state at low fields but high temperatures. It is further argued on this basis that the first-order decoupling transition terminates at a critical endpoint at a temperature of order the 2D vortex-lattice melting temperature and at a perpendicular field of order many times the dimensional cross-over scale B_{\perp}^* . The resulting phase diagram (Fig. 1) is strikingly similar to those reported for the mixed phase of clean high-temperature superconductors.^{2,3,5–7}

The paper is organized in the following way. Section II contains the weak-coupling duality analysis of the uniformly frustrated XY model. The principal input is the nature of the phase coherence in isolated layers, which is assumed to be either quasi long range [Eq. (17)] or short range [Eq. (18)]. The output of the weak-coupling analysis is that the former implies the presence of a Josephson effect, whereas the latter implies its absence. Equations (43) and (55) for the local Josephson coupling in the respective coupled and decoupled phases summarize these results. This theory is then used to determine the phase diagram of extremely type-II layered superconductors in perpendicular magnetic field in section III. The principal new result is the prediction of a coupled 2D vortex lattice phase

at low temperatures and high fields that notably displays a Josephson plasma resonance with exponential temperature dependence [see Fig. 1 and Eq. (66)]. A comparison of these results with previous experimental and theoretical work is made in section IV, while some conclusions are reached in section V. Finally, technical issues that concern the long-range nature of phase correlations in the 2D XY model and that concern a fermion analogy employed to describe the Josephson coupling between layers are treated in Appendix A and B, respectively.

II. Theory

The thermodynamics in the interior of the mixed phase of extremely type-II superconductors ($\lambda_L \rightarrow \infty$) can be described at least qualitatively by the uniformly frustrated XY model over the cubic lattice.^{14,15,24} In the case where the superconductor is composed of N Josephson coupled layers, the corresponding kinetic energy for the superfluid flow reads

$$\begin{aligned}
 E_{XY}^{(3)} = & -J_{\parallel} \sum_{l=1}^N \sum_{\vec{r}} \sum_{\mu=x,y} \cos[\Delta_{\mu}\phi(\vec{r}, l) - A_{\mu}(\vec{r}, l)] \\
 & - J_{\perp} \sum_{l=1}^{N-1} \sum_{\vec{r}} \cos[\phi(\vec{r}, l+1) - \phi(\vec{r}, l) - A_z(\vec{r}, l)]. \quad (1)
 \end{aligned}$$

Above, $\phi(\vec{r}, l)$ is the superconducting phase at a point \vec{r} in layer l , while $A_{\mu} = (0, b_{\perp}x, -b_{\parallel}x)$ is the vector potential. Also, Δ_{μ} denotes the nearest-neighbor difference operator along the $\hat{\mu}$ direction of the square lattice. The magnetic induction parallel and perpendicular to the layers is related to the frustration \vec{b} through the respective identities $B_{\parallel} = (\Phi_0/2\pi d)b_{\parallel}$ and $B_{\perp} = (\Phi_0/2\pi a)b_{\perp}$. Here the length scales d and a denote respectively the separation between adjacent layers and the lattice constant for each square-lattice layer. The latter is of order the superconducting coherence length at zero temperature. Also, $J_{\parallel} = (d/4\pi)(\Phi_0/2\pi\lambda_L)^2$ is the local phase rigidity within layers, while J_{\perp}/a^2 denotes the local Josephson coupling energy per unit area. It is important to observe that the Josephson penetration length at zero temperature, $\gamma'_0 a$, provides a natural scale for the XY model (1) in the limit of weak coupling between layers, in which case the model anisotropy parameter $\gamma'_0 = (J_{\parallel}/J_{\perp})^{1/2}$ is much larger than unity.⁴ This shall be assumed throughout.

Last, we remind the reader that any generalized phase auto-correlation function set by an integer source field, $p(r)$, is related to the corresponding partition function

$$Z_{XY}^{(3)}[p] = \int \mathcal{D}\phi e^{-E_{XY}^{(3)}/k_B T} e^{i \sum p\phi} \quad (2)$$

by the quotient^{17,18}

$$\left\langle \exp \left[i \sum_r p(r)\phi(r) \right] \right\rangle = Z_{XY}^{(3)}[p]/Z_{XY}^{(3)}[0]. \quad (3)$$

A knowledge of these amplitudes characterizes the thermodynamics of the layered XY model (1).

A. Layered Coulomb Gas. We shall now employ the well-known dual representation of the XY model (1) that is based on the Fourier series expansion¹⁸

$$e^{\beta \cos \theta} = \sum_{n=-\infty}^{\infty} I_{|n|}(\beta) e^{in\theta}$$

of the Gibbs distribution in terms of the modified Bessel functions $I_n(x)$. This identity allows the phase variables to be integrated out of the partition function at the price of introducing a new integer field n that lives on each link of the XY model (1). Substitution into Eq. (2) thereby results in the dual form

$$Z_{XY}^{(3)}[p] = I_0^{\mathcal{N}'}(\beta_{\perp}) I_0^{2\mathcal{N}}(\beta_{\parallel}) \sum_{\{n_{\mu}(r)\}} \Pi_r \delta \left[\sum_{\nu} \Delta_{\nu} n_{\nu}|_r - p(r) \right] \cdot \Pi_{r,\nu} t_{n_{\nu}(r)}(\beta_{\nu}) e^{-in_{\nu}(r)A_{\nu}(r)} \quad (4)$$

expressed in terms of modified Bessel functions and the quotients $t_n(\beta) = I_{|n|}(\beta)/I_0(\beta)$. Above, $n_{\mu}(r)$ is an integer link-field on the layered lattice structure of points $r = (\vec{r}, l)$, with $\mu = \hat{x}, \hat{y}, \hat{z}$, and $\beta_{\mu} = J_{\mu}/k_B T$. Also, \mathcal{N} denotes the total number of sites, while $\mathcal{N}' = \mathcal{N}(1 - N^{-1})$ gives the total number of rungs between layers. [The perpendicular link fields at the boundary layers are set to $n_z(\vec{r}, 0) = 0 = n_z(\vec{r}, N)$]. We now take the crucial step in the theory by observing that only the configurations with $n_z(r) = 0, \pm 1$ are relevant in the weak-coupling limit,^{35,36} $\beta_{\perp} \ll 1$. After re summation over the parallel link fields n_x and n_y in Eq. (4), we then obtain the form

$$Z_{XY}^{(3)}[p] = I_0^{\mathcal{N}'}(\beta_{\perp}) \sum_{\{n_z(r)\}} y_0^{N[n_z]} \cdot \Pi_{l=1}^N Z_{XY}^{(2)}[ql] \cdot e^{-i \sum_r n_z A_z} \quad (5)$$

for the partition function of the 3D XY model in terms of sums of products over partition functions

$$Z_{XY}^{(2)}[q_l] = \int \mathcal{D}\phi_l e^{-E_{XY}^{(2)}/k_B T} e^{i \sum q_l \phi_l} \quad (6)$$

for frustrated 2D XY layers in isolation, where

$$E_{XY}^{(2)} = -J_{\parallel} \sum_{\vec{r}} \sum_{\mu=x,y} \cos[\Delta_{\mu} \phi_l(\vec{r}) - A_{\mu}(\vec{r})] \quad (7)$$

is the intra-layer superfluid kinetic energy, and where

$$q_l(\vec{r}) = p(\vec{r}, l) + n_z(\vec{r}, l - 1) - n_z(\vec{r}, l) \quad (8)$$

is the source integer field. Above also, $N[n_z] = \sum_{\vec{r}, l} |n_z(\vec{r}, l)|$ is the number of n_z (fluxon) charges per configuration and $y_0 = I_1(\beta_{\perp})/I_0(\beta_{\perp})$ is the bare fugacity. The latter tends to

$$y_0 = \beta_{\perp}/2 \quad (9)$$

in the weak-coupling limit $\beta_{\perp} \ll 1$. By analogy with Eq. (3), we now identify the quotient $Z_{XY}^{(2)}[q_l]/Z_{XY}^{(2)}[0]$ with the generalized auto-correlation function

$$C_l[q_l] = \left\langle \exp \left[i \sum_{\vec{r}} q_l(\vec{r}) \phi(\vec{r}, l) \right] \right\rangle_{J_{\perp}=0} \quad (10)$$

of the 2D XY model with frustration.^{17,18} Comparison with Eqs. (5) and (6) thus yields the form

$$Z_{XY}^{(3)}[p] = I_0^{\mathcal{N}'}(\beta_{\perp}) \cdot Z_{CG}[p] \cdot \Pi_{l=1}^N Z_{XY}^{(2)}[0] \quad (11)$$

for the partition function of the layered XY model in terms of a product of a layered Coulomb gas ensemble

$$Z_{CG}[p] = \sum_{\{n_z(r)\}} y_0^{N[n_z]} \cdot \Pi_{l=1}^N C_l[q_l] \cdot e^{-i \sum_r n_z A_z} \quad (12)$$

with N XY model layers in isolation (see ref. 27). This is the final result of taking the selective high-temperature limit, $y_0 \rightarrow 0$, which is assumed throughout.

Before proceeding further, we now derive a useful relation between the density of n_z charges and the local Josephson coupling. Eq. (1) indicates that the latter is given by

$$\langle \cos \phi_{l,l+1} \rangle = \mathcal{N}'^{-1} \partial \ln Z_{XY}^{(3)}[0] / \partial \beta_{\perp}, \quad (13)$$

where $\phi_{l,l+1}(\vec{r}) = \phi(\vec{r}, l+1) - \phi(\vec{r}, l) - A_z(\vec{r})$ is the gauge-invariant phase difference between consecutive layers. Yet the Coulomb-gas ensemble (12) yields the identity $\langle N[n_z] \rangle = y_0(\partial \ln Z_{\text{CG}}[0]/\partial y_0)$ for the total number of fluxons on average. By the factorization (11) for the layered XY model, we thereby obtain the general expression

$$\langle N[n_z] \rangle / \mathcal{N}' = 2y_0(\langle \cos \phi_{l,l+1} \rangle - y_0) \quad (14)$$

for this quantity per rung in terms of the local Josephson coupling.

To demonstrate that (12) is indeed a layered Coulomb gas ensemble, consider now a single neutral pair of unit n_z charges that lie in between layers l' and $l' + 1$ in the absence of an external source, $p = 0$, with the negative and positive charges located at planar sites \vec{r}_1 and \vec{r}_2 , respectively. This represents the first non-trivial term in the selective high-temperature expansion (12). The gauge-invariant product over intra-layer autocorrelation functions in the layered Coulomb gas ensemble then reduces to the product $C_l(\vec{r}_1, \vec{r}_2)C_{l'+1}^*(\vec{r}_1, \vec{r}_2)$ of the corresponding two-point functions,

$$C_l(\vec{r}_1, \vec{r}_2) = \left\langle \exp \left[i\phi(\vec{r}_1, l) - i\phi(\vec{r}_2, l) \right] \right\rangle_{J_\perp=0}, \quad (15)$$

within isolated layers. This function takes the form

$$C_l(\vec{r}_1, \vec{r}_2) = |C_l(\vec{r}_1 - \vec{r}_2)| e^{-i \int_1^2 \vec{A}'(\vec{r}) \cdot d\vec{r}} \quad (16)$$

in terms of a suitably gauge-transformed vector potential \vec{A}' , and in terms of a magnitude that varies with the separation as

$$|C_l(\vec{r})| = g_0(r_0/|\vec{r}|)^{\eta_{2D}} \quad \text{for} \quad |\vec{r}| \ll \xi_{\text{vx}}, \quad (17)$$

and as

$$|C_l(\vec{r})| = g_0 \exp(-|\vec{r}|/\xi_{\text{vx}}) \quad \text{for} \quad |\vec{r}| \gg \xi_{\text{vx}}. \quad (18)$$

Here,

$$\eta_{2D} = \eta_{\text{sw}} + \eta_{\text{vx}} \quad (19)$$

is the 2D correlation exponent inside layer l , where $\eta_{\text{sw}} = (2\pi\beta_\parallel)^{-1}$ and η_{vx} are the respective spin-wave and vortex contributions (see Appendix A). Also, ξ_{vx} denotes the 2D phase correlation length, while the length $r_0 = a_{\text{vx}}/2^{3/2}e^{\gamma_E}$ is set by the inter-vortex scale,

$$a_{\text{vx}} = (\Phi_0/B_\perp)^{1/2}, \quad (20)$$

and by Euler's constant,¹⁸ γ_E . General scaling considerations³⁷ indicate that the ratio $\xi_{\text{vx}}/a_{\text{vx}}$ depends only on temperature. Last, the prefactor in expression (17) is of order $g_0 \sim (a/a_{\text{vx}})^{\eta_{\text{sw}}}$. At fields $B_{\perp} > \Phi_0/\gamma_0'^2 a^2$, it is therefore of order unity for anisotropy parameters, $\gamma_0' < e^{2\pi\beta_{\parallel}}$, that are not astronomically large. The effective layered CG ensemble (12) therefore takes form¹⁹

$$Z_{\text{CG}}[0] \cong \sum_{\{n_z\}} y^{N[n_z]} \exp \left\{ -\frac{1}{2} \sum_l \sum_{\vec{r}_1 \neq \vec{r}_2}' q_l(\vec{r}_1) \left[\eta_{2D} \ln(r_0/|\vec{r}_1 - \vec{r}_2|) - V_{\text{string}}^{[q_l]}(\vec{r}_1, \vec{r}_2) \right] q_l(\vec{r}_2) - i \sum_l \sum_{\vec{r}}' n_z(\vec{r}, l) A_z(\vec{r}, l) \right\} \quad (21)$$

in the limit of dilute fluxon (n_z) charges. Above, the Coulomb gas ensemble (12) has been coarse grained up to the natural ultra-violet scale a_{vx} . In particular, the sums above are restricted to a square sublattice with lattice constant a_{vx} . This requires the introduction of an effective coarse-grained fugacity

$$y = g_0 (a_{\text{vx}}/a)^2 y_0. \quad (22)$$

At relatively small separations, $|\vec{r}_1 - \vec{r}_2| \ll \xi_{\text{vx}}$, within a 2D correlation length, the fluxons experience a pure ($V_{\text{string}}^{[q_l]} = 0$) Coulomb interaction set by η_{2D} [see Eq. (17)]. At large separations $|\vec{r}_1 - \vec{r}_2| \gg \xi_{\text{vx}}$, on the other hand, the fluxons experience a pure ($\eta_{2D} = 0$) confining interaction $V_{\text{string}}^{[q_l]}(\vec{r}_1, \vec{r}_2) = |\vec{r}_1 - \vec{r}_2|/\xi_{\text{vx}}$ [see Eq. (18) and refs. 35, 38 and 39]. Study of the asymptotic behavior exhibited by general n -point auto-correlation functions (10) for the 2D XY model reveals that the form (21) for the Coulomb gas ensemble (12) remains valid in the case of a general fluxon charge configuration, $n_z(\vec{r}, l)$ (see Appendix A). However, the preceding confining interaction exists only between those well separated points \vec{r}_1 and \vec{r}_2 in a given layer l that are connected by a string.

The coarse-graining (21) of the original Coulomb gas ensemble (12) assumes implicitly that there be no more than one $n_z = \pm 1$ charge per unit sublattice area a_{vx}^2 . This is equivalent to the condition $\langle N[n_z] \rangle / \mathcal{N}' < a^2/a_{\text{vx}}^2$ for the density of such fluxons. Comparison with expression (14) for this density then implies that the preceding condition is satisfied at temperatures and fields such that $\beta_{\perp} a_{\text{vx}}^2/a^2 < 1$. The validity of the above coarse-grained Coulomb-gas ensemble (21) is hence assured at high perpendicular fields $B_{\perp} > \beta_{\parallel} \Phi_0/\gamma_0'^2 a^2$. Below, we determine the thermodynamic nature of the two phases

that correspond to quasi long-range (17) and to short-range (18) phase correlations within isolated layers.

B. Coupled Phase. Consider first the case (17) where quasi long-range intra-layer phase correlations are present: $\xi_{vx} = \infty$ and $V_{\text{string}}^{[q]} = 0$. Inter-layer n_z charges in the Coulomb gas ensemble are screened at low temperatures, $\eta_{2D} < 2$. Global charge conservation is no longer enforced in this instance. Let us also assume the weak-coupling regime defined by the inequality $y \ll 1$ to be satisfied by the effective fugacity (22) of the coarse-grained CG ensemble (21). Following the standard prescription,^{35,36} we then sum *independently* over charge configurations at each site, with the restriction to values $n_z = 0, \pm 1$. An appropriate Hubbard-Stratonovich transformation²⁴ of the CG (21) in the absence of a source ($p = 0$) followed by a Debye-Hückel type of approximation^{35,36} reveals that it is equal to the corresponding one

$$Z_{\text{LD}}[0] = \int \mathcal{D}\theta e^{-E_{\text{LD}}/k_B T} \quad (23)$$

for a renormalized Lawrence-Doniach (LD) model⁴ up to a factor that depends only on β_{\parallel} . The LD energy functional

$$E_{\text{LD}} = \bar{J}_{\parallel} \sum_{l=1}^N \sum_{\mu=x,y} \sum_{\vec{r}}' \frac{1}{2} (\Delta'_{\mu} \theta_l)^2 - 2y k_B T \sum_{l=1}^{N-1} \sum_{\vec{r}}' \cos(\theta_{l+1} - \theta_l - A_z) \quad (24)$$

is summed over the coarse-grained sublattice. Here,

$$\bar{J}_{\parallel} = k_B T / 2\pi \eta_{2D} \quad (25)$$

is the macroscopic phase rigidity of an isolated layer.⁴⁰ (The validity of the Debye-Hückel type approximation will be established *a posteriori*.) Taking the continuum limit of the lattice energy (24) yields the more familiar expression

$$E_{\text{LD}} = \bar{J}_{\parallel} \int d^2 r \left[\sum_{l=1}^N \frac{1}{2} (\vec{\nabla} \theta_l)^2 - \Lambda_0^{-2} \sum_{l=1}^{N-1} \cos(\theta_{l+1} - \theta_l - A_z) \right] \quad (26)$$

for the energy functional of the LD model, with a renormalized Josephson penetration length

$$\Lambda_0 = a(\bar{\beta}_{\parallel} / 2g_0 y_0)^{1/2}, \quad (27)$$

expressed in terms of the parameter $\bar{\beta}_{\parallel} = \bar{J}_{\parallel}/k_B T$. Substitution of the bare fugacity (9) that corresponds to the conventional XY model yields a more familiar expression

$$\Lambda_0 = a(\bar{J}_{\parallel}/g_0 J_{\perp})^{1/2} \quad (28)$$

for the renormalized Josephson scale. The above continuum description (26) is understood to have an ultraviolet cut off $\alpha_0 \sim a_{\text{vx}}$ on the order of the coarse-grained sub-lattice constant. It is also *gaussian* within layers, which means that parallel Josephson vortices are the only topological excitations that it contains explicitly.

The above renormalized LD model is known to be macroscopically Josephson coupled at temperatures below $k_B T_{*0} = 4\pi\bar{J}_{\parallel}$.^{21–24,41,42} To illustrate this fact, consider first the minimal double-layer case, $N = 2$. The zero-temperature line tension of a single Josephson vortex is equal to the linear energy density

$$\varepsilon_{\parallel}(0) = 2^{5/2}\bar{J}_{\parallel}/\Lambda_0 \quad (29)$$

of a sine-Gordon soliton.²⁴ The condensation energy, on the other hand, is in general equal to $-G_{\text{cond}} = k_B T \ln Z_{\text{LD}}$. At zero temperature and zero parallel field, this energy per vertical rung is thus given by

$$-G_{\text{cond}}^{(0)}(0)/\mathcal{N}' = \bar{J}_{\parallel} a^2 / \Lambda_0^2. \quad (30)$$

At the unbinding temperature $k_B T_{\text{LE}} = 2\pi\bar{J}_{\parallel}$ for Josephson vortex/anti-vortex pairs,^{41,42} on the other hand, the double-layer LD model can be analyzed exactly through a mapping to ideal spinless fermions (see Appendix B). The line-tension so obtained is given by the expression

$$\varepsilon_{\parallel}(T_{\text{LE}}) = \pi\bar{J}_{\parallel}\alpha_0/\Lambda_0^2, \quad (31)$$

where α_0 is the natural ultraviolet length scale of order the underlying lattice constant a_{vx} for LD model (26). This mapping can similarly be employed to obtain the expression

$$-G_{\text{cond}}^{(0)}(T_{\text{LE}})/\mathcal{N}' = (\bar{J}_{\parallel}/8)(a\alpha_0/\Lambda_0^2)^2 \quad (32)$$

for the condensation energy at zero parallel field. Notice that both the line-tension and the condensation energy above are renormalized down with respect to their zero-temperature

values by factors of α_0/Λ_0 . Finally, both the fermion analogy⁴² (see Appendix B) and the original CG ensemble (21) indicate that the renormalized LD model (26) decouples at $k_B T_* \cong 4\pi\bar{J}_\parallel$.^{21–24} The fermion analogy in particular yields that both the line tension $\varepsilon_\parallel(T)$ and the condensation energy $G_{\text{cond}}^{(0)}(T)$ vanish in an exponentially activated fashion as T approaches T_* from below (see Appendix B). A “semi-classical” calculation⁴³ of the renormalization to the zero-temperature line tension ε_\parallel that results from thermal wandering of the Josephson vortex is consistent with the exact results listed above at the three temperatures $T = 0, T_{\text{LE}}$, and T_* .²⁴ This calculation obtains a line-tension of the form

$$\varepsilon_\parallel = 4\bar{J}_\parallel/\lambda_J, \quad (33)$$

where λ_J is a renormalized Josephson penetration length that varies with temperature following

$$\frac{\lambda_J}{r_0} = \left(\frac{\Lambda_0}{2^{1/2}r_0} \right)^{[1-(\eta_{2D}/2)]^{-1}}. \quad (34)$$

The exponent above takes the values 1, 2 and ∞ at the respective temperatures $T = 0, T_{\text{LE}}$, and T_* . This agrees with Eqs. (29), and (31) if the ultraviolet length scales are identified by $r_0 = (\pi/8)\alpha_0$. It is also consistent with a decoupling transition at T_* .

Given the success of the “semi-classical” result [Eqs. (33) and (34)] for the line-tension in the double-layer case, we propose that the condensation energy per vertical rung of the sine-Gordon model [Eq. (26) for $N = 2$] generally takes the form

$$-G_{\text{cond}}^{(0)}/\mathcal{N}' = h_0\bar{J}_\parallel a^2/2\lambda_J^2 \quad (35)$$

in zero parallel field, where h_0 is weakly temperature (η_{2D}) dependent and of order unity. Comparison with Eqs. (30) and (32), for example, yields the assignments $h_0(0) = 1$ and $h_0(T_{\text{LE}}) = 4/\pi^2$ for this prefactor. Since the Gibbs free energy of a double-layer is generally given by the formula

$$G_{\text{cond}} \cong G_{\text{cond}}^{(0)} + (L_x L_y d)(|B_\parallel|/\Phi_0)\varepsilon_\parallel \quad (36)$$

in the limit of vanishingly small parallel field, B_\parallel , we obtain the final result

$$-G_{\text{cond}}/\mathcal{N}' \cong \bar{J}_\parallel \left[\frac{1}{2}h_0(a/\lambda_J)^2 - 4(a/\lambda_J)(ad|B_\parallel|/\Phi_0) \right] \quad (37)$$

for the condensation energy in such case. We shall now make use of this result in order to compute the local Josephson coupling (13). Since we have the identity $Z_{\text{CG}}[0] = Z_{\text{LD}}[0]$ up to a factor independent of β_{\perp} , the factorization (11) implies that

$$\langle \cos \phi_{l,l+1} \rangle = y_0 + \partial(-G_{\text{cond}}/\mathcal{N}'k_B T)/\partial\beta_{\perp}. \quad (38)$$

Substitution of the double-layer result (37) for the Gibbs free energy above yields the final expression

$$\langle \cos \phi_{l,l+1} \rangle \cong y_0 + h_0 g_0 \nu \left(\frac{2r_0^2}{\Lambda_0^2} \right)^{\nu-1} - h_1 g_0 \nu \left(\frac{2^{1/2} r_0}{\Lambda_0} \right)^{\nu-1} \cdot \frac{|B_{\parallel}|}{B_{\parallel}^*} \quad (39)$$

for the local Josephson coupling in the limit of small parallel fields, where

$$\nu = [1 - (\eta_{2D}/2)]^{-1} \quad (40)$$

is the temperature dependent exponent that appears in Eq. (34), where $B_{\parallel}^* = \Phi_0/\Lambda_0 d$ is the crossover field above which Josephson vortices overlap, and where $h_1 = 2^{3/2}$. The second term on the right-hand side of Eq. (39) agrees with the result obtained by Glazman and Koshelev⁴⁴ for the local Josephson coupling in layered superconductors at zero field ($r_0 \sim a$).

Consider next the renormalized LD model (26) in the case of an infinite number of layers, $N \rightarrow \infty$. The zero-temperature condensation energy at $B_{\parallel} = 0$ is clearly equal to that of the previous double-layer case (30). In addition, mean-field treatments of the fermion analogy for the renormalized LD model indicate that the Gibbs free energy G_{cond} at low parallel fields is in general given by the original energy functional (26),⁴² but with a renormalized Josephson penetration length $\lambda_J(T) > \Lambda_0$. In the continuum limit, we have for example

$$G_{\text{cond}} \cong G_{\text{cond}}^{(0)}(0) + \frac{\bar{J}_{\parallel}}{2d} \int dx dy dz \left[\left(\frac{\partial \theta}{\partial x} \right)^2 + \left(\frac{\partial \theta}{\partial y} \right)^2 + \gamma^{-2} \left(\frac{\partial \theta}{\partial z} - \frac{A_z}{d} \right)^2 \right], \quad (41)$$

with the effective mass anisotropy parameter $\gamma = \lambda_J/d$. The line-tension of a single parallel Josephson vortex in the present case $N \rightarrow \infty$ is then given by the known result⁴

$$\varepsilon_{\parallel} \cong (\pi \bar{J}_{\parallel} / \lambda_J) \ln(\lambda_L/d). \quad (42)$$

Here, the resulting logarithmically divergent integral (41) has been cut off by the London penetration length, λ_L , which is taken to be the natural infrared scale. Also, the condensation energy in the absence of parallel field is then given by the zero-temperature result, Eq. (30), but with the bare Josephson scale Λ_0 replaced by $\lambda_J(T)$. If we now assume that $\lambda_J(T)$ has the same scaling form⁴⁴ as the analogous scale in the double-layer case, Eq. (34), then a repetition of the previous steps yields an expression for the local Josephson coupling in the presence of a small parallel field of the form

$$\langle \cos \phi_{l,l+1} \rangle \cong \frac{1}{2} \beta_{\perp} + f_0 \left(\frac{r_0}{\Lambda_J} \right)^{\eta} - f_1 \left(\frac{r_0}{\Lambda_J} \right)^{\eta/2} \cdot \frac{|B_{\parallel}|}{B_{\parallel}^*}. \quad (43)$$

Here $r_0 = a_{\text{vx}}/2^{3/2}e^{\gamma_E}$, Λ_J is of order Λ_0 , and the prefactor f_1 is of order $g_0 \ln(\lambda_L/d)$. This result for the local Josephson coupling is corroborated by the observation that the second-term above coincides with the intra-layer auto-correlation function (17) evaluated at a separation $r = \Lambda_J$ of order $\Lambda_0 = \gamma_0 \cdot d$!⁴⁴ This suggests that the prefactor and the exponent for the second term have the limiting values $\eta \rightarrow \eta_{2D}$ and $f_0 \rightarrow g_0$ at low temperatures, $\eta_{2D} \ll 1$, which is corroborated by the double-layer result (39). The latter corresponds to the assignments $\eta = (\eta_{2D}^{-1} - \frac{1}{2})^{-1}$ for the effective exponent,⁴⁴ $\Lambda_J = \Lambda_0/2^{1/2}$ for the effective anisotropy scale, and $f_i = h_i g_0 / (1 - \frac{1}{2} \eta_{2D})$ for the prefactors ($i = 0, 1$). Notice that $f_0(0) = g_0$ and $f_0(T_{\text{LE}}) = (8/\pi^2)g_0$ in this case, which indicates that f_0/g_0 is close to unity at low temperatures $\eta_{2D} \ll 1$.

We now demonstrate the validity of the Debye-Hückel type of approximation referred to earlier. In passing from the layered CG ensemble (21) to the renormalized LD model (24), the amplitudes $1+2y \cos(\theta_{l+1} - \theta_l - A_z)$ that appear in the partition function as a result of the Hubbard-Stratonovich transformation²⁴ are replaced by $\exp[2y \cos(\theta_{l+1} - \theta_l - A_z)]$ (see refs. 35 and 36). This is valid as long as Debye screening of the fluxon charges occurs, which requires many such charges within a screening cloud: $\pi \lambda_J^2 \cdot \langle N[n_z] \rangle / \mathcal{N}' a^2 > 1$. Study of the previous formulas in the double-layer case, Eqs. (14), (34), and (39), yields the result $\frac{\pi}{2}(f_0/g_0)\bar{\beta}_{\parallel}$ for the former quantity. The Debye-Hückel type approximation is therefore valid at low temperatures $k_B T < \bar{J}_{\parallel}$, which as we shall see in the next section contains the present coupled phase.

Last, we shall compute the perpendicular phase rigidity, $\rho_s^{\perp} = \frac{\partial^2}{\partial A_z'^2} (G_{\text{cond}}/\mathcal{N})|_0$ in the coupled phase. Here, A_z' represents the longitudinal component of the vector potential that

is assumed to be equal across all of the perpendicular links. Periodic boundary conditions in the direction perpendicular to the layers are implicit. First, the duality transformation (4) yields the general expression

$$\rho_s^\perp = \mathcal{N}^{-1} \left\langle \left[\sum_{\vec{r}, l} n_z(\vec{r}, l) \right]^2 \right\rangle k_B T \quad (44)$$

for the perpendicular stiffness in terms of a fluxon average over the dual ensemble (21). Yet the n_z charges are screened in the coupled phase. Such short-range correlations among the fluxons suggests the approximation $\mathcal{N}^{-1} \langle [\sum_{\vec{r}, l} n_z(\vec{r}, l)]^2 \rangle \cong \langle n_z^2 \rangle$ for the average that appears above. But since the fluxon charges are effectively restricted to take values $n_z = 0, \pm 1$ in the selective high-temperature limit, $y_0 \rightarrow 0$, we also have approximately that $\langle n_z^2 \rangle \cong \langle N[n_z] \rangle / \mathcal{N}'$. Use of Eq. (14) thus yields the (mean-field) estimate

$$\rho_s^\perp / J_\perp \cong \langle \cos \phi_{l, l+1} \rangle - y_0 \quad (45)$$

for the perpendicular phase rigidity of the uniformly frustrated layered XY model in the selective high-temperature limit of the coupled phase. Comparison with the previous results for the local Josephson coupling indicates that the perpendicular phase rigidity decreases with increasing temperature and field following the sum of the last two terms on the right-hand side of Eq. (43).

In conclusion, a macroscopic Josephson effect exists at low temperatures, $\eta_{2D} < 2$, in extremely type-II layered superconductors if isolated layers display quasi-long-range order (17). Indeed, the analysis just completed demonstrates that this is the case even in the weak-coupling regime $\langle \cos \phi_{l, l+1} \rangle \ll 1$ of the coupled phase reached at high perpendicular fields $B_\perp \gg \Phi_0 / \gamma_0'^2 a^2$.

C. Decoupled Phase. Consider next the case (18) in which intra-layer correlations are short range: $\xi_{vx} < \infty$. Although the coarse-grained form (21) of the Coulomb gas ensemble remains valid in this instance, a direct analysis starting from the original form for the ensemble defined by Eqs. (8) and (12) is more expeditious. Since the phase auto-correlation functions (3) of interest are those that probe inter-layer couplings, the associated source field shall be assumed to take the form

$$p(\vec{r}, l) = n_z^{(0)}(\vec{r}, l - 1) - n_z^{(0)}(\vec{r}, l), \quad (46)$$

where $n_z^{(0)}(r)$ is a fixed fluxon “charge impurity” field. Notice that the intra-layer sources (8) can then be simply re-expressed in terms of the net fluxon charge distribution

$$m_z = n_z^{(0)} + n_z \quad (47)$$

as

$$q_l(\vec{r}) = m_z(\vec{r}, l-1) - m_z(\vec{r}, l). \quad (48)$$

This image of fluxon charge impurities is useful in the calculation of inter-layer autocorrelators. In particular, Eqs. (3), (11) and (12) yield the identity

$$\left\langle \exp\left(i \sum_r [p(r)\phi(r) - n_z^{(0)}(r)A_z(r)]\right) \right\rangle = Z'_{\text{CG}}[p]/Z_{\text{CG}}[0] \quad (49)$$

between the corresponding gauge-invariant quantity and the quotient of the modified partition function

$$Z'_{\text{CG}}[p] = \sum_{\{n_z(r)\}} y_0^{N[n_z]} \cdot \prod_{l=1}^N C_l[q_l] \cdot e^{-i \sum_r m_z A_z} \quad (50)$$

with the unmodified one (12) in the absence of a source. We shall now apply this to the calculation of the local Josephson coupling $\langle e^{i\phi_{l,l+1}} \rangle$, which corresponds to fixing a unit fluxon “charge impurity” at some point in between layers l and $l+1$. In the selective high-temperature limit, $y_0 \rightarrow 0$, the configurations that contribute to the numerator (50) of the quotient are limited to those with a net fluxon charge $-N[n_z] = -1$ in between layers l and $l+1$ only. Likewise, the denominator $Z_{\text{CG}}[0]$ can be approximated by unity in such case. We thereby obtain Koshelev’s formula^{10,11}

$$\langle e^{i\phi_{l,l+1}} \rangle \cong y_0 \int d^2r C_l(0, \vec{r}) C_{l+1}^*(0, \vec{r}) e^{-ib_{\parallel} x/a^2} \quad (51)$$

for the local Josephson coupling in the decoupled phase. Notice that short-range autocorrelations (18) yield a finite integral above, while quasi-long-range autocorrelations (17) yield a divergent integral for 2D correlation exponents that satisfy $\eta_{2D} < 1$. Last, Eq. (51) also implies that the first derivative $\partial \langle e^{i\phi_{l,l+1}} \rangle / \partial B_{\parallel}$ of the local Josephson coupling is null in zero parallel field. This result survives to all orders of the selective high-temperature expansion in the decoupled phase. Eq. (38) in turn implies that the condensation energy satisfies $\partial^2 G_{\text{cond}} / \partial \beta_{\perp} \partial B_{\parallel} = 0$ at $B_{\parallel} = 0$. We then have a null line tension for Josephson

vortices in the decoupled phase, since the latter yields $\varepsilon_{\parallel} = 0 = \varepsilon_{\parallel}|_{J_{\perp}=0}$. In conclusion, the Josephson effect is absent in the weak-coupling limit of extremely type-II layered superconductors when the intra-layer phase correlations of isolated layers are short range.

We shall now demonstrate that phase auto-correlations in between layers are short-range in the decoupled phase. Since the introduction of parallel magnetic field generally reduces inter-layer phase correlation [see Eq. (55) below], it is sufficient to consider the zero-field case, $B_{\parallel} = 0$. By the previous discussion, the gauge-invariant phase autocorrelator $\langle e^{i\phi_{l,l+n}} \rangle$ in between $n + 1$ adjacent layers is equivalent to fixing a column made up of $n \geq 1$ unit fluxon “charge impurities” in between layers l and $l + n$. The lowest order configurations that contribute to the numerator (50) of the CG ensemble are those with net fluxon charge $-N[n_z] = -n$ distributed evenly in between layers l and $l + n$ only. Equations (16), (49) and (50) therefore yield the expression

$$\langle e^{i\phi_{l,l+n}} \rangle = (y_0/a^2)^n \prod_{l'=l}^{l+n} \left[\int d^2 r_{l'} |C_{l'}(\vec{r}_{l'})| \right] e^{i \int_l^{l+n} \vec{A}'(\vec{r}) \cdot d\vec{r}} \delta^{(2)}(\vec{r}_l + \vec{r}_{l+1} + \dots + \vec{r}_{l+n}) \quad (52)$$

for this quantity to lowest order in the fugacity. Substitution of the Fourier representation $\delta^{(2)}(\vec{R}) = (2\pi)^{-2} \int d^2 q e^{i\vec{q} \cdot \vec{R}}$ for the 2D δ -function above in addition to replacing the phase factor by unity then yields the inequality

$$\langle e^{i\phi_{l,l+n}} \rangle \leq \left[\mathcal{C}_0 \int \frac{d^2 q}{(2\pi)^2} \left(\frac{\mathcal{C}_q}{\mathcal{C}_0} \right)^{n+1} \right] (y_0 \mathcal{C}_0 / a^2)^n, \quad (53)$$

where

$$\mathcal{C}_q = \int d^2 r |C_{l'}(\vec{r}_{l'})| e^{i\vec{q} \cdot \vec{r}_{l'}} \quad (54)$$

is the Fourier transform of the intra-layer autocorrelator. The latter are assumed to be identical for each layer. [Equation (53) is an equality in the absence of field, $B_{\perp} = 0$, or for $n = 1$.] The prefactor in brackets above (53) typically decays polynomially with n [see Eq. (56) below]. We then conclude that the inter-layer autocorrelator $\langle e^{i\phi_{l,l+n}} \rangle$ decays at least exponentially with n in the weak-coupling limit $y_0 \rightarrow 0$. This implies that the macroscopic phase rigidity, ρ_s^{\perp} , in the direction perpendicular to the layers is null in the decoupled phase. Notice that such a null result is consistent with expression (44) and with the fluxon charge neutrality that is characteristic of the decoupled phase.

To get a more concrete idea of the results just obtained in the selective high-temperature limit, $y_0 \rightarrow 0$, for the decoupled phase, we shall now assume the form (16) and (18) for the short-range intra-layer autocorrelator. Substitution into (51) yields the expression

$$\langle \cos \phi_{l,l+1} \rangle \cong \frac{\pi}{2} \left[1 + \left(\frac{b_{\parallel} \xi_{vx}}{2} \right)^2 \right]^{-3/2} \left(\frac{\xi_{vx}}{a_{vx}} \right)^2 g_0 y \quad (55)$$

for the local Josephson coupling in parallel field. Notice the anti-cyclotronic $1/B_{\perp}$ dependence and $1/T$ dependence in the above expression for the local Josephson coupling that is generally expected from Koshelev's formula (51). Notice also the quadratic dependence with parallel field that is consistent with a null parallel line tension, $\varepsilon_{\parallel} = 0$. It is interesting to remark that outside of the 2D critical regime, where $\xi_{vx} \sim a_{vx}$, the result (55) coincides with the form (43) for the local Josephson coupling in the coupled phase. The corresponding exponent $\eta = 2$ occurs precisely at the depinning temperature, $\eta_{2D} = 1$, for Josephson vortices in the double-layer case (39)!⁴² Last, the inter-layer autocorrelator satisfies Eq. (53), with Fourier components $C_q = 2\pi g_0 \xi_{vx}^2 / (q^2 \xi_{vx}^2 + 1)^{3/2}$ for the short-range correlations (18). We thereby obtain the inequality

$$\langle e^{i\phi_{l,l+n}} \rangle \leq \frac{g_0}{3n+1} (2\pi y \xi_{vx}^2 / a_{vx}^2)^n \quad (56)$$

for the autocorrelator in between $n+1$ layers in the weak-coupling limit of the decoupled phase.

III. Mixed Phase

We shall now employ the theory developed in the preceding section for a finite number N of Josephson-coupled XY layers (1) with uniform frustration^{14,15,24} to determine the thermodynamic nature of the mixed phase in the corresponding extremely type-II layered superconductor. The Josephson energy will be assumed to follow the temperature dependence $J_{\perp} \propto T_{c0} - T$ in the vicinity of the mean-field critical temperature,⁴⁵ T_{c0} , while the anisotropy parameter $\gamma'_0 = (J_{\parallel}/J_{\perp})^{1/2}$ will be assumed to be a constant that is large compared to unity.

A. Phase Boundaries. Consider first the limit of weak local Josephson coupling, $\langle \cos \phi_{l,l+1} \rangle \rightarrow 0$. Comparison with the results (43) and (55) indicates that this limit

coincides with the regime of high temperatures and high fields, $T \gg T_J = J_\perp/k_B$ and $B_\perp \gg B_\perp^* = \Phi_0/\Lambda_0^2$. It is well known that an isolated lattice of 2D vortices (6) melts at a temperature

$$k_B T_m^{(2D)} \cong J_\parallel/20, \quad (57)$$

above which quasi long-range positional correlation is lost.^{29–31} The transition is driven by the unbinding of dislocation pairs and it is second-order.^{32,33} This is reflected by the analysis of the Villain model (Appendix A), where the elementary excitations are explicitly interstitial/vacancy pairs with respect to the triangular vortex lattice that exists at zero temperature.^{12,13} Suppose now that the inter-layer coupling is weak enough so that the inequality $T_J \ll T_m^{(2D)}$ is satisfied. (This is consistent with a minimum anisotropy parameter γ'_0 between four and five.) Let us also make the plausible assumption that the phase correlations within an isolated layer inherit the quasi long-range behavior shown by the vortex positions at low temperature.^{29,30} By the analysis of the previous section, we then conclude that the layers exhibit a macroscopic Josephson effect at low temperature $T < T_m^{(2D)}$ following the renormalized LD model (26), while they decouple at high temperature $T > T_m^{(2D)}$. In the limit of high perpendicular fields, which coincides with the present weak-coupling limit $\gamma'_0 \rightarrow \infty$ at fixed field, we therefore have a low-temperature phase composed of N 2D vortex lattices that exhibit a Josephson effect, and that is separated from a decoupled vortex liquid phase at high temperatures by a second-order line at $T = T_m^{(2D)}$. Hence, neither the Friedel scenario²⁵ (decoupled superconducting layers) nor the “line-liquid” state^{14,24,26} (coupled normal layers) are thermodynamically possible in the weak-coupling limit.

Consider next the weak-coupling regime at small yet non-vanishing local Josephson coupling, $\langle \cos \phi_{l,l+1} \rangle \ll 1$. It is important to observe first that the selective high-temperature expansion for the local Josephson coupling in the decoupled phase breaks down at perpendicular fields of order the scale

$$B_\perp^\times = g_0^2 \beta_\parallel (\xi_{vx}/a_{vx})^2 B_\perp^* \quad (58)$$

in the absence of parallel field. The corresponding approximation (55) is of order unity in such case, which coincides roughly with the identification of length scales $\xi_{vx} \sim \Lambda_0$. The selective high-temperature expansion (43) for the coupled phase, on the other hand, breaks

down at much lower fields of order B_{\perp}^* for temperatures $T \lesssim T_m^{(2D)}$. For a given temperature inside the decoupled phase, the confining nature of the CG (12) is most prominent at perpendicular fields that are much larger than B_{\perp}^{\times} . In particular, the string interaction (18) binds together dilute fluxon-antifluxon pairs into stable dipoles of dimension ξ_{vx} that do not overlap in this limit. The regime is best described physically by a decoupled vortex liquid with short-range correlations on the scale of ξ_{vx} .¹⁰ At weak-coupling, $\langle \cos \phi_{l,l+1} \rangle \ll 1$, Eq. (55) indicates that the effective fugacity y of the CG ensemble (21) is small compared to unity. Eq. (55) also implies that the cross-over temperature T_{\times} for a fixed perpendicular field B_{\perp} (58) lies inside of the 2D critical regime ($\xi_{vx} \gg a_{vx}$) in such case. A similar dilute CG description (21) exists for the layered XY model *without* frustration, in which case coarse-graining is absent, $a_{vx} \rightarrow a$, and the effective fugacity y is replaced by the bare one, y_0 .²⁰ By analogy, we therefore conclude that a *second-order* melting transition takes place at a temperature T_m that lies inside of the dimensional crossover window $T_m^{(2D)} < T < T_{\times}$ for a fixed perpendicular field $B_{\perp} \gg B_{\perp}^*$ (see ref. 34). It is worth pointing out that the bound fluxon pairs begin to overlap inside of this regime [see Eq. (62) below].

Before we continue, it is useful first to define a decoupling contour

$$\langle \cos \phi_{l,l+1} \rangle = \langle \cos \phi_{l,l+1} \rangle_D \quad (59)$$

in the T - B_{\perp} plane for fixed parallel field, B_{\parallel} . Here, $\langle \cos \phi_{l,l+1} \rangle_D$ is a constant less than but of order unity.^{11,46} Its value will be determined *a posteriori* below. In particular, the result (43) for the local Josephson coupling in the coupled phase yields (i) a nearly “vertical” contour line at temperatures of order the Josephson energy, $k_B T_J = J_{\perp}$, in the limit of extremely high perpendicular fields B_{\perp} compared to B_{\perp}^* , and (ii) a contour line at higher temperatures $T_J \ll T < T_m^{(2D)}$ with a perpendicular field that increases exponentially with T_{*0}/T as

$$H_D \sim B_{\perp}^* (f_0 / \langle \cos \phi_{l,l+1} \rangle_D)^{2/\eta}. \quad (60)$$

In the decoupled phase at high temperatures outside of the 2D critical region ($\xi_{vx} \sim a_{vx}$), on the other hand, the result (55) for the local Josephson coupling indicates that the decoupling contour lies at a perpendicular field

$$H_D \sim g_0^2 \beta_{\parallel} B_{\perp}^* / \langle \cos \phi_{l,l+1} \rangle_D \quad (61)$$

that decreases monotonically with temperature as $1/T$. A similar result for the decoupling transition is obtained using the elastic medium description.^{8,9} Since this high-temperature contour should connect smoothly with the low-temperature one (60) in the coupled phase, the contour line (59) must *cross* the 2D melting line $T = T_m^{(2D)}$ at a perpendicular field many times B_\perp^* .

Suppose now that the local Josephson coupling, $\langle \cos \phi_{l,l+1} \rangle$, begins to approach unity, which can be achieved by either lowering the perpendicular field or the temperature. The selective high-temperature expansion in the coupled phase (43) breaks down at temperatures and fields in the vicinity of the decoupling contour (59). Yet the CG ensemble (21) is screened in the Josephson-coupled phase at low temperatures $T < T_m^{(2D)}$ for small effective fugacity y . The neutral plasma of fluxons is dilute in this instance by Eq. (14). Since an increase in the fluxon density with respect to the dilute limit can only increase the effect of screening, then no thermodynamic phase transition is possible as a function of field (y) for $T < T_m^{(2D)}$. This general argument is corroborated by the phase diagram for the neutral 2D Coulomb gas.⁴⁷ The break-down of the selective high-temperature expansion in the coupled phase that occurs in the vicinity of the decoupling contour (59) must therefore signal a crossover into a flux-line lattice regime.

On the other hand, what happens in the decoupled phase as the perpendicular field is lowered through the cross-over field B_\perp^\times at temperatures and fields that are beyond the 2D critical regime ($\xi_{vx} \sim a_{vx}$)? It is useful in this case to determine first the point at which bound fluxon-antifluxon pairs begin to overlap. Since the average fluxon occupation per vertical rung is equal to $2a^2/r_s^2$, where r_s denotes the average spacing in between dipoles, and since the second term in expression (14) for this quantity is negligible when the local Josephson coupling is of order unity, we then have

$$\xi_{vx}^2/r_s^2 \cong y_0(\xi_{vx}^2/a^2)\langle \cos \phi_{l,l+1} \rangle. \quad (62)$$

Notice that the prefactor on the right-hand side above is of order the high-temperature approximation (55) for the local Josephson coupling. Since both the approximate (55) and the true value for $\langle \cos \phi_{l,l+1} \rangle$ are of order unity^{11,46} along the decoupling contour (59) at temperatures outside of the 2D critical regime, Eq. (62) then indicates that the fluxon pairs begin to overlap ($r_s \sim \xi_{vx}$) in such case. The dipoles disassociate, however, once they overlap due to the ineffectiveness of the string (18). The system must therefore

eventually experience a (inverted) phase transition into a screened CG above a critical coupling $\langle \cos \phi_{l,l+1} \rangle_D$ less than but of order unity.^{11,46} Also, the phase transition must be first-order since there is no diverging length scale nearby ($\xi_{vx} \sim a_{vx}$).⁴⁸ This is consistent with elastic medium descriptions of the vortex lattice in layered superconductors,⁹ which also predict a first-order decoupling transition at a perpendicular field H_D of order (61). Last, continuity with the second-order melting/decoupling transition that takes place at higher fields implies that this first-order decoupling line must end where the former line begins. We therefore predict a critical endpoint at a temperature and field of order $T_m^{(2D)}$ and many times B_\perp^* , respectively.

Finally, the layered XY model (1) shows a second-order phase transition in the absence of frustration at a relatively large critical temperature $k_B T_c \sim J_\parallel$ in comparison to the 2D melting temperature (57).³⁴ The above first-order decoupling line must therefore end in the vicinity of this zero-field critical point as temperature increases. Also, the previous duality analysis can be repeated in its entirety for the zero-field case, where the replacement $a_{vx} \rightarrow a$ must be made globally.²⁰ Eqs. (43) and (55) then imply that the local Josephson coupling is of order unity at temperatures between $T_J = J_\perp/k_B$ and $\min[2\pi\bar{J}_\parallel/k_B \ln \gamma'_0, T_c^{(2D)}]$. We therefore have $T_D < T_c$, which is also consistent with the second critical endpoint in the vicinity of T_c at zero field.

The above results are summarized by the phase diagram shown in Fig. 1. The phenomenology⁴⁵ $J_\perp = E_{J0}(T_{c0} - T)/T_{c0}$ for the Josephson energy in the vicinity of the zero-field transition at T_{c0} yields the linear temperature dependence^{2,8,9} $H_D(T) = \gamma_2^{-2} H_{c2}(T)$ for the first-order decoupling field (61), where $H_{c2}(T) \sim (\Phi_0/a^2)(T_{c0} - T)/T$ is the mean-field perpendicular upper-critical field, and where $\gamma_2 \sim \langle \cos \phi_{l,l+1} \rangle_D^{1/2} \cdot (k_B T_{c0}/E_{J0})^{1/2}$ is an effective anisotropy parameter. The selective high-temperature expansion (55) indicates that this decoupling line is depressed quadratically by parallel field at temperatures outside of the 2D critical regime. Such behavior is consistent with anisotropic Ginzburg-Landau theory.⁴⁹ Continuity with the contour (60) in the coupled phase also indicates that the first-order line crosses the second-order melting line, $T = T_m$. The phase boundary then continues up in field along the latter second-order line. Finally, Eq. (43) implies that the decoupling contour (59) continues into the coupled phase at temperatures $T < T_m$ down to the Josephson energy scale T_J . The non-zero line tension (42) for Josephson

vortices that is characteristic of the coupled phase results in a *linear* depression of this contour with parallel field [see Eq. (43) and ref. 50]. Last, it is possible that a vestige of the second-order melting transition found at high fields $B_{\perp} > B_{\perp}^*$ persists down into the low-field region in the form of a crossover (see Fig. 1). This regime, however, is beyond the scope of the weak-coupling approach elaborated here.

B. Latent Heat and Josephson Plasma Resonance. We shall now estimate the latent heat across the first-order decoupling line (59). The perpendicular contribution is equal to $\Delta E_{\perp}/\mathcal{N}' = -J_{\perp}\Delta\langle\cos\phi_{l,l+1}\rangle$. The corresponding entropy jump is then equal to $\Delta S_{\perp} = \Delta E_{\perp}/T$. The entropy jump per vortex, $a_{\text{vx}}^2\Delta S_{\perp}/\mathcal{N}'a^2$, at the first-order transition due to the Josephson coupling is therefore given by

$$\Delta S_{\perp} \text{ per vx} = \beta_{\parallel}(B_{\perp}^*/H_D)(-\Delta\langle\cos\phi_{l,l+1}\rangle)k_B. \quad (63)$$

Eq. (61) implies that it is of order $-\Delta\langle\cos\phi_{l,l+1}\rangle k_B$. Last, it is perhaps useful to point out that a jump

$$\Delta\langle N[n_z]\rangle/\mathcal{N}' = \beta_{\perp}\Delta\langle\cos\phi_{l,l+1}\rangle \quad (64)$$

in the number of inter-layer fluxons per rung at the first-order decoupling transition is implied by the relation (14).

Apart from playing an important role in the determination of the phase diagram discussed above, the local Josephson coupling between layers can also be directly probed through *c*-axis Josephson plasma resonance (JPR) experiments. Theory dictates that the plasma frequency is given by $\omega_{pl} = \omega_0\langle\cos\phi_{l,l+1}\rangle^{1/2}$, where ω_0 is its zero-field value.^{10,11,46} The local Josephson coupling is given by Eq. (55) in the vortex liquid phase, where $\xi_{\text{vx}} \sim a_{\text{vx}}$. This yields Koshelev's result^{10,11}

$$(\omega_{pl}/\omega_0)^2 \cong (f_0\Phi_0/B_{\perp}a^2)(J_{\perp}/2k_B T) \quad (65)$$

for the corresponding JPR contours at constant frequency $\omega_{pl} \ll \omega_0$, where f_0 is weakly temperature dependent and of order unity (g_0^2). Consider next the coupled phase at perpendicular fields in the weak-coupling regime $a \ll a_{\text{vx}} \ll \Lambda_0$. The second term on the right-hand side of Eq. (43) for the local Josephson coupling is then dominant. The vortex contribution to the 2D correlation exponent (19) can be neglected in the low-temperature limit [see Appendix A, Eq. (A8)]. We therefore obtain the corresponding JPR contours

$$(\omega_{pl}/\omega_0)^2 \cong f_0(B_J/B_{\perp})^{T/T^*0} \quad (66)$$

at constant frequency in the coupled phase at low temperatures, $T_J \ll T < T_m^{(2D)}$, where B_J is a constant perpendicular field scale of order B_\perp^* . Notice then that the perpendicular field along a given contour diverges *exponentially* with T_{*0}/T in the weak-coupling regime, $\omega_{pl} \ll \omega_0$ [see also Eq. (60)].

C. Bulk Limit. The thermodynamic limit, $N \rightarrow \infty$, of an infinite number of layers must be taken in order to model extremely type-II layered superconductors in bulk. Since the decoupling contour (59) is determined primarily by the Josephson coupling in between adjacent layers, it should not change much in the case of an infinite number of layers. The first-order decoupling transition should therefore survive the bulk limit.⁵¹ With respect to the question of the survival of the second order melting line in the bulk limit, it is useful to observe that the Coulomb gas ensemble (21) used here to describe the frustrated XY model also describes the unfrustrated model if one makes the replacement $a_{vx} \rightarrow a$ for the natural ultraviolet scale. Yet it is obvious that the universality class of the unfrustrated XY model should pass from 2D to 3D as $N \rightarrow \infty$. Given that both the frustrated and unfrustrated layered XY models have a common Coulomb gas form (21), then the universality class of the former should pass from the 2D to the 3D universality class of the latter as $N \rightarrow \infty$. In other words, the second-order melting line should survive the bulk limit as well.

D. Bulk Pinning. Vortices both in real superconductors and in the XY model (1) can be pinned, respectively, by defects and by the underlying cubic lattice at low enough temperatures. To get an idea of how pinning can effect the Josephson coupling, we shall consider the optimal case where each c-axis flux line is *fixed* to some type of a correlated pin. The latter could represent a twin boundary, a columnar track, or a model substrate potential. If we now return to the analysis of the CG ensemble (21), this means (i) that the auto-correlation functions (16)-(18) for each layer in isolation are all identical, and (ii) that they resemble the auto-correlation function of the *unfrustrated* XY model on the square lattice due to the fact that vortex fluctuations are suppressed. In particular, they show quasi-long range order ($\xi_{vx} = \infty$) at temperatures below the vortex/anti-vortex unbinding transition, $k_B T_c^{(2D)} = \frac{\pi}{2} J_\parallel$, following Eq. (17). The phase autocorrelations within isolated layers are short range ($\xi_{vx} < \infty$) at high temperatures $T > T_c^{(2D)}$, on the other hand, following Eq. (18). The previous analysis holds in general, with the exception that the Coulomb gas ensemble (21) is *not* coarse grained. In particular, the

replacement $a_{v\chi} \rightarrow a$ must be made globally. This yields a *field-independent* result for the local Josephson coupling (13). No first-order phase transition is therefore expected. A second-order decoupling transition, however, remains at a critical temperature T_c that should lie within the dimensional crossover window $T_c^{(2D)} < T < T_\times$ (see ref. 34). By the previous arguments, its universality class should pass from that of the 2D XY model without frustration to that of the 3D one in the thermodynamic limit of an infinite number of layers. A schematic phase diagram that summarizes the above results is shown in Fig. 2.

It must be emphasized that the above results are obtained under the assumption of optimum correlated pinning, which may not be realizable at all temperatures and fields. Indeed, an isolated 2D vortex lattice within the XY model is pinned only at low temperatures $T < T_{dp}^{(2D)}$ inside of the quasi-ordered phase below the 2D melting temperature $T_m^{(2D)}$.^{29,30} The 2D depinning temperature, $T_{dp}^{(2D)}$, is null in the zero-field limit, and it increases linearly with increasing field. This depinning line, furthermore, merges with the 2D melting line $T = T_m^{(2D)}$ at a field of order $\Phi_0/36a^2$. Since the focus of this paper is the mixed phase of type-II superconductors, which effectively have no substrate potential, we shall defer the analysis of intra-layer intrinsic pinning effects in the XY model (1) to future work.

IV. Discussion

Below, we shall compare the results obtained in the previous sections for the thermodynamics of the mixed phase in extremely type-II layered superconductors with numerical simulations of the frustrated XY model, with relevant experimental work on high-temperature superconductors, and with the flux-line entanglement ideas developed by Nelson⁵² and co-workers.¹³

A. Numerical Simulations. Let us first review the Monte Carlo simulation results that have been obtained recently for the uniformly frustrated XY model on an isolated square lattice.²⁹ Both these and simulations of the associated lattice Coulomb gas³⁰ find a vortex-lattice melting transition at a temperature (57) that is independent of field, in accord with theoretical expectations.³¹ They also find, however, that pinning due to the square-lattice

grid at commensurate flux densities can only be neglected at large inter-vortex scales

$$a_{\text{vx}} > 6a. \quad (67)$$

(See the discussion at the end of section III.D.) Monte Carlo simulations of the layered XY model (1) have also been performed.¹⁴ The most extensive simulations find evidence for a single first-order phase transition that coincides with the decoupling contour (59).¹⁵ The results reported in ref. 11, for example, yield a value for $\langle \cos \phi_{l,l+1} \rangle_D$ near 1/2. These simulations find no evidence for a critical endpoint where the first-order transition terminates with decreasing temperature, however, contrary to the theoretical results obtained here (see Fig. 1).

The cause for the above discrepancy may have two sources. First, the coarse-grained Coulomb-gas ensemble (21) used here to analyze the coupled phase at low temperatures may not be valid in regimes where the 2D vortex lattices are pinned by the XY model grid. This suggests that comparison of theory with the Monte Carlo simulations of the layered XY model (1) should be restricted to low perpendicular fields (67). Second, the phase diagram shown in Fig. 1 is valid only for anisotropy parameters inside of the range

$$5 < \gamma'_0 < L/2\pi a \quad (68)$$

for XY layers of dimensions L by L . The lower bound guarantees the inequality $T_J < T_m^{(2D)}$, while the upper bound insures that the system is not effectively decoupled at zero temperature.³⁴ Most, if not all of the Monte Carlo simulations performed to date have not satisfied conditions (67) and (68) simultaneously. This indicates that a comparison with the present theory is premature.

B. High- T_c Superconductivity. The phase diagram shown in Fig. 1 for the layered XY model is consistent with the nature of the flux-lattice melting observed in the mixed phase of clean high-temperature superconductors.¹⁻³ The latter melting transition begins at (or near) the zero field critical point, but it terminates in the middle of the $T - H_\perp$ plane as the temperature is lowered. The multi-critical point obtained here at $T_0 \sim T_m^{(2D)}$ and $H_0 \gtrsim B_\perp^*$ is roughly consistent with this effect. It must be remarked, however, that the location of the critical endpoint observed experimentally in high-temperature superconductors is sensitive to the degree of disorder.⁵

The critical endpoint for the vortex-lattice melting line observed in clean high-temperature superconductors also coincides with a multi-critical point. In particular, the flux-line lattice frees itself from pins through thermal fluctuations across a vertical line in the $T - H_{\perp}$ plane that extends up from the critical endpoint.^{5,6} The combination of surface barriers plus the second-order vortex-lattice melting transition at $T = T_m$ that is obtained here theoretically for extremely type-II layered superconductors could account for this effect (see Fig. 1 and ref. 1).

A so-called *second peak* line also extends horizontally to lower temperatures in the $T - H_{\perp}$ plane from the critical endpoint in clean high-temperature superconductors.⁷ Bulk pinning is observed to increase dramatically at perpendicular fields that lie above this line. Recent observations of muon spin resonance (μ SR) in the same systems have reached similar conclusions.⁵³ It is conceivable that this effect is related to the dimensional cross-over transition that is predicted here in the coupled phase between a flux-line lattice phase at low fields and a smectic solid phase at high fields (see Fig. 1). In particular, point pinning is relatively more effective in the latter phase composed of weakly coupled 2D vortex lattices. Note, however, that the cross-over predicted here for a finite number of layers in the absence of pins is possibly broad [see Eq. (60)], whereas the second peak transition is sharp.⁵⁻⁷ This suggests either that a true decoupling phase transition occurs in bulk (see ref. 51), or that point pins are what drive the second-peak phenomenon into a sharp transition.⁵³

C. Topological Defects and Flux-line Entanglement. Distinct solid phases of vortex matter have been proposed in the past.⁴ In particular, Frey, Nelson and Fisher have presented arguments for the existence of a “supersolid” phase in the mixed phase of layered superconductors that is characterized by highly entangled flux lines that preserve the 2D lattice structure within layers.¹³ The “supersolid” phase is predicted to occur whenever the temperature, T_d , above which interstitial/vacancy pairs proliferate¹² lies below the melting temperature, T_m , of the quasi-2D vortex lattice. The phase composed of Josephson-coupled 2D vortex lattices that appears at low temperatures and high fields in the phase diagram for the layered XY model displayed in Fig. 1 evidently has physical characteristics that coincide with the “supersolid” phase.⁵¹ In particular, the flux arrangement is ordered within planes yet disordered along the field direction. The quasi-2D solid phase discussed here is

furthermore limited to temperatures inside of the window $T_D < T < T_m$ at relatively high fields $H_\perp \gg B_\perp^*$. If the (Josephson) decoupling temperature scale T_D is then identified with the scale T_d , at which point vacancy/interstitial pairs begin to proliferate,¹² we recover precisely the “supersolid” regime that is discussed in ref. 13. Last, we remark that an interstitial/vacancy pair in a single layer is confined by Josephson vortices that run between the neighboring layers.¹² This indicates that J_\perp is the limiting energy scale for such defects. This in turn makes the identification of T_D with T_d plausible, since $k_B T_D$ is also of order the Josephson scale J_\perp in the high-field limit by Eqs. (43) and (59).

V. Concluding Remarks

A schematic phase diagram (Fig. 1) for the mixed phase of extremely type-II layered superconductors has been proposed on the basis of a weak-coupling duality analysis of the layered XY model with uniform frustration (1). The artificial pinning effects that arise from the 2D model grid in each layer were effectively removed by a coarse-graining (21) of the resulting dual Coulomb gas description (12). We notably predict that a smectic (super¹³) solid type of vortex matter exists at high fields and low temperatures, and that this phase undergoes a second-order melting transition into a vortex liquid phase at higher temperatures. The solid phase exhibits a macroscopic Josephson effect, while the liquid phase does not. The weak-coupling analysis thus indicates that neither an intermediate “line-liquid” phase that exhibits a macroscopic Josephson effect between normal layers, nor a Friedel scenario characterized by decoupled superconducting layers, are thermodynamically possible in pure extremely type-II superconductors. It has also been argued that the second-order melting transition converts itself into a first-order one at lower fields of order many times the dimensional cross-over scale, B_\perp^* . This potentially accounts for the critical endpoint for the first-order melting of the flux-line lattice that is observed in clean high-temperature superconductors.^{1–3}

Notably absent in this theory are effects due to magnetic screening⁵⁴ and to disorder caused by point pins.⁵⁵ Both of these effects are present to some degree in the mixed phase of all high-temperature superconductors.^{5,7} It remains to be seen how such departures from the pure XY model description (1) for the mixed phase of extremely type-II layered superconductors may change the conclusions reached above.

The author is grateful for the hospitality of the Instituto de Ciencia de Materiales de Madrid, where part of this work was completed, and to Nestor Parga and Charles Creffield for discussions. He is also indebted to Lev Bulaevskii for pressing him to compute the “cosine”.

Appendix A: Villain Model

The duality analysis for the conventional XY model presented in section II can be repeated in its entirety for the case the XY model in the Villain form:

$$Z_V^{(3)}[p] = \sum_{\{n_\nu(r)\}} \prod_r \delta \left[\sum_\nu \Delta_\nu n_\nu |_r - p(r) \right] \exp \left[- \sum_r \left(\frac{1}{2\beta_\parallel} \vec{n}^2 + \frac{1}{2\beta_\perp} n_z^2 + i \sum_\nu n_\nu A_\nu \right) \right]. \quad (A1)$$

In the weak-coupling limit, $\beta_\perp \rightarrow 0$, partial resummation of the type outlined at the beginning of section II.A yields the factorized form

$$Z_V^{(3)}[p] = Z_{\text{CG}}[p] \cdot \prod_{i=1}^N Z_V^{(2)}[0] \quad (A2)$$

for the partition function in terms of the corresponding 2D partition functions

$$Z_V^{(2)}[q_l] = \sum_{\{\vec{n}\}} \prod_{\vec{r}} \delta[\vec{\nabla} \cdot \vec{n}|_{\vec{r},l} - q_l(\vec{r})] \times \exp \left[- \frac{1}{2\beta_\parallel} \sum_{\vec{r}} \vec{n}^2(\vec{r}, l) - i \sum_{\vec{r}} \vec{n}(\vec{r}, l) \cdot \vec{A}(\vec{r}) \right] \quad (A3)$$

and the Coulomb gas ensemble (12). In contrast with the case of the conventional XY model, the fugacity is now equal to

$$y_0 = e^{-1/2\beta_\perp}, \quad (A4)$$

while the 2D auto-correlation functions (10) are set by the quotients

$$C_l[q_l] = Z_V^{(2)}[q_l] / Z_V^{(2)}[0]. \quad (A5)$$

Repeating the derivation of the renormalized LD model (26) results in a renormalized Josephson penetration length (27) that displays an artificial temperature dependence acquired from the fugacity (A4). Also, Koshelev's formula (51) indicates that the local Josephson coupling acquires the same artificial temperature dependence in the decoupled phase.

The above results were initially derived in ref. 19 by following an alternate route, where the spin-wave and the vortex degrees of freedom within layers are explicit. The

Villain model displays a complete factorization of such degrees of freedom. This permits the 2D auto-correlation functions (A5) to be computed analytically in the low-temperature ordered phase (see refs. 17 and 18). For example, the two-point auto-correlation function (15) for an isolated layer l has the asymptotic form

$$\langle e^{i\phi(\vec{r}_1,l)} e^{-i\phi(\vec{r}_2,l)} \rangle_{J_\perp=0} = g_0 \left(\frac{r_0}{r_{12}} \right)^{\eta_{2D}} e^{-i \int_1^2 \vec{A}'(\vec{r}) \cdot d\vec{r}} \quad (\text{A6})$$

in the ordered phase as a function of the separation $r_{12} = |\vec{r}_1 - \vec{r}_2|$, where A' is a suitably gauge-transformed vector potential, where $\eta_{2D} = \eta_{\text{sw}} + \eta_{\text{vx}}$ is the 2D correlation exponent, and where r_0 is of order the natural ultra-violet length scale a_{vx} set by the spacing between vortices. The latter is in accord with general scaling considerations.³⁷ The separate spin-wave and vortex components of η_{2D} are given by

$$\eta_{\text{sw}} = (2\pi\beta_{\parallel})^{-1} \quad (\text{A7})$$

and by

$$\eta_{\text{vx}} = -\frac{\pi}{4a^2} \sum_{\vec{r} \neq 0} |\vec{r}|^2 \langle \delta Q_l(0) \delta Q_l(\vec{r}) \rangle_{\text{vx}}, \quad (\text{A8})$$

respectively, where $\delta Q_l(\vec{r}) = Q_l(\vec{r}) - Q_0(\vec{r})$ is the deviation of the intra-layer vorticity $Q_l(\vec{r})$ at the dual site \vec{r} in layer l with respect to the flux-line lattice, $Q_0(\vec{r})$, that threads each and every layer at zero temperature. (Surface barriers are assumed.) The result (A8) is obtained through a cumulant expansion of the dipole pairs so indicated over a 2D Coulomb gas (vx) with a uniform background charge density $\langle Q_l \rangle / a^2 = b_\perp / 2\pi a$ and a temperature of η_{sw} . Last, the prefactor in expression (A6) is of order

$$g_0 \sim (a/a_{\text{vx}})^{\eta_{\text{sw}}}. \quad (\text{A9})$$

The upper bound $\gamma'_0 < e^{2\pi\beta_{\parallel}}$ on the anisotropy parameter guarantees that g_0 be of order unity for perpendicular fields $B_\perp > B_\perp^*$.

The methods used to compute the above two-point function (A6) in the ordered phase can be extended to compute the asymptotic form of any general n -point autocorrelation function (10). One thereby obtains the result

$$|C_l[q_l]| = g_0^{n+(l)} \exp \left[\frac{1}{2} \sum_{\vec{r}_1 \neq \vec{r}_2} \eta_{2D} \cdot q_l(\vec{r}_1) \ln(|\vec{r}_1 - \vec{r}_2|/r_0) q_l(\vec{r}_2) \right], \quad (\text{A10})$$

where $n_+(l)$ denotes the number of positive (or negative) probe charges applied to layer l . Notice that this expression is equal to the product of two factors, each corresponding to the spin-wave and to the vortex components of the 2D correlation exponent η_{2D} . The vortex factor in the generalized auto-correlation function (10) is obtained through the cumulant expansion of the associated Coulomb gas ensemble mentioned above [see Eq. (A8) and refs. 17 and 18].

With respect to the evaluation of the 2D auto-correlation function in the disordered phase at high temperatures, it is more useful to study the original dual form (A3) for the corresponding partition function, $Z_V^{(2)}(\vec{r}_1, \vec{r}_2)$. The image of a string with its ends tied to the points \vec{r}_1 and \vec{r}_2 at a low dual temperature β_{\parallel} indicates the form

$$Z_V^{(2)}(\vec{r}_1, \vec{r}_2) \propto e^{-\sigma_{\parallel} r_{12}/\beta_{\parallel}} e^{-i \int_1^2 \vec{A}(\vec{r}) \cdot d\vec{r}}$$

for the latter, where σ_{\parallel} denotes the string tension (see refs. 35, 38 and 39). We thereby obtain the asymptotic result

$$\langle e^{i\phi(\vec{r}_1, l)} e^{-i\phi(\vec{r}_2, l)} \rangle_{J_{\perp}=0} = g_0 e^{-r_{12}/\xi_{vx}} e^{-i \int_1^2 \vec{A}(\vec{r}) \cdot d\vec{r}} \quad (A11)$$

for the auto-correlation function of the 2D Villain model in the disordered phase, where $\xi_{vx} = \beta_{\parallel}/\sigma_{\parallel}$ is the correlation length. The string image can also be used to compute general n -point autocorrelation functions (10) in the limit where the probe charges correspond to well separated dipoles. The autocorrelator in such case is simply given by the product of the two-point functions (A11) represented by each dipole.

Appendix B: Fermion Analogy

We shall now determine the thermodynamic character of the renormalized LD model [Eqs. (25)-(27)] in parallel magnetic field $B_{l,l+1} = (\Phi_0/2\pi d)b_{l,l+1}$ in between layers l and $l + 1$. This model is defined by the energy functional

$$E_{\text{LD}} = \bar{J}_{\parallel} \int d^2r \left\{ \sum_{l=1}^N \frac{1}{2} (\vec{\nabla} \theta_l)^2 - \Lambda_0^{-2} \sum_{l=1}^{N-1} \cos[\theta_{l+1}(\vec{r}) - \theta_l(\vec{r}) + b_{l,l+1}x] \right\} \quad (B1)$$

of the real phase variable $\theta_l(\vec{r})$. It is known to be equivalent to coupled chains of spinless fermions at zero temperature, where each chain corresponds to a layer.^{41,42} (Previous analogies for layered superconductors in parallel field employed fermions that live *in between* consecutive layers.^{56,57}) Specifically, the Hamiltonian for the fermion model is divided into intra-chain and inter-chain pieces, $H = H_{\parallel} + H_{\perp}$, with respectively

$$H_{\parallel} = \sum_{l=1}^N \int dx \left[v_{\text{F}} \left(\Psi_L^{\dagger} i \partial_x \Psi_L - \Psi_R^{\dagger} i \partial_x \Psi_R \right) + U_{\parallel} \Psi_L^{\dagger} \Psi_R^{\dagger} \Psi_L \Psi_R \right] \quad (B2)$$

and

$$H_{\perp} = U_{\perp} \sum_{l=1}^{N-1} \int dx \left[\Psi_L^{\dagger}(x, l) \Psi_R^{\dagger}(x, l+1) \Psi_L(x, l+1) \Psi_R(x, l) + \text{H.c.} \right]. \quad (B3)$$

Above, $\Psi_R(x, l)$ and $\Psi_L(x, l)$ represent the field operators for right (R) and left (L) moving fermions. The coordinate along the Josephson vortices, y , is related to the imaginary time variable τ of the fermion analogy by $y = v'_{\text{F}} \tau$. Here, the Fermi velocity $v'_{\text{F}} = v_{\text{F}} \text{sech } 2\phi$ is renormalized by the intra-chain interaction U_{\parallel} ,⁵⁸ with $\tanh 2\phi = U_{\parallel}/2\pi v_{\text{F}}$. Also, $U_{\perp} > 0$ is a repulsive backscattering interaction energy⁵⁸ in between chains. The Gibbs free-energy of the LD model (B1) with respect to the normal state is then found to be related to the ground-state energy E_{F} of the fermion analogy by

$$G_{\text{cond}}/k_{\text{B}}T = (L_y/v'_{\text{F}})[E_{\text{F}}(U_{\perp}) - E_{\text{F}}(0)]. \quad (B4)$$

The identifications

$$b_{l,l+1} = 2\pi(N_{l+1} - N_l)/L_x, \quad (B5)$$

$$\eta_{2D} = 2e^{2\phi}, \quad (B6)$$

$$\Lambda_0^{-2} = \alpha_0^{-2} (|U_{\perp}|/\pi v'_{\text{F}}) \eta_{2D}, \quad (B7)$$

complete the equivalence between the models, where N_l/L_x gives the fermion density in the l^{th} chain, where $\eta_{2D} = k_B T / 2\pi \bar{J}_{\parallel}$ is the 2D correlation exponent, and where α_0 is the natural ultraviolet length scale of the LD model (B1). [Note that the above fermion analogy can directly be shown to be equivalent to the CG ensemble (21) in the screened phase, $\xi_{\text{vx}} = \infty$, without recourse to the renormalized LD model (B1) (see ref. 41).]

Consider first the minimal case of $N = 2$ layers. The above analogy then reduces to a Luther-Emery (LE) model for pseudo spin-1/2 fermions,⁵⁸ which exhibits pseudo spin-charge separation. The right-moving and left-moving spinless fermions corresponding to the pseudo-spin sector, $a_k^{\dagger}|0\rangle$ and $b_k^{\dagger}|0\rangle$, are governed by an ideal Hamiltonian along the Luther-Emery line $\eta_{2D} = 1$ of the form $H_{\sigma} = \sum_k [v'_F k (a_k^{\dagger} a_k - b_k^{\dagger} b_k) + \Delta_{\sigma} a_k^{\dagger} b_k + \Delta_{\sigma}^* b_k^{\dagger} a_k]$. They exhibit a spectrum $\varepsilon_{\sigma}^{\pm}(k) = \pm(v'_F k^2 + \Delta_{\sigma}^2)^{1/2}$ that is characterized by a pseudo spin gap

$$\Delta_{\sigma} = U_{\perp} / 2\pi\alpha_0. \quad (B8)$$

In the absence of parallel field, $b_{1,2}$, the hole band ($-$) is filled and the particle band ($+$) is empty. Since the pseudo-charge sector is independent of the coupling between chains, U_{\perp} , the groundstate energy density relative to the decoupled state, $U_{\perp} = 0$, is therefore equal to

$$[E_{\text{F}}(U_{\perp}) - E_{\text{F}}(0)]/L_x = -\Delta_{\sigma}^2 / 4\pi v'_F. \quad (B9)$$

(The logarithmically divergent contribution above that is equal to $L_x^{-1} \sum_k \Delta_{\sigma} \langle a_k^{\dagger} b_k \rangle$ has been removed by a normal-ordering type of procedure.) By Eq. (B4), the condensation energy per vertical rung at the corresponding LE temperature, $k_B T_{\text{LE}} = 2\pi \bar{J}_{\parallel}$, is then equal to

$$-G_{\text{cond}}^{(0)}(T_{\text{LE}})/\mathcal{N}' = (a\Delta_{\sigma}/v'_F)^2 (\bar{J}_{\parallel}/2) \quad (B10)$$

in zero parallel field. Yet in the limit of vanishingly small parallel field, the Gibbs free energy takes the form given by Eq. (36), where ε_{\parallel} denotes the line tension for a single Josephson vortex. It is known that single-particle excitations within chains inherit the pseudo spin gap (B8) because of spin-charge separation. In addition, Eq. (B5) indicates that adding or removing a fermion from one of the two chains is equivalent to injecting a Josephson vortex in between the two superconducting layers. The equivalence formula (B4) thus yields the identity

$$\varepsilon_{\parallel}(T_{\text{LE}}) = (|\Delta_{\sigma}|/v'_F) k_B T_{\text{LE}} \quad (B11)$$

in between the line-tension and the pseudo spin gap. Comparison with Eqs. (B7) and (B8) yields the final expressions

$$-G_{\text{cond}}^{(0)}(T_{\text{LE}})/\mathcal{N}' = (a\alpha_0/\Lambda_0^2)^2(\bar{J}_{\parallel}/8) \quad (\text{B12})$$

and

$$\varepsilon_{\parallel}(T_{\text{LE}}) = \pi\bar{J}_{\parallel}\alpha_0/\Lambda_0^2 \quad (\text{B13})$$

for the above free energies in terms of the original model (B1) parameters.

At arbitrary number of layers and at arbitrary temperatures, the fermion analogy can be treated in the mean-field approximation defined by the charge-density wave (CDW) order parameter $\chi_l(x) = \langle \Psi_R^\dagger(x, l)\Psi_L(x, l) \rangle$ and the associated gap equation⁴² $\Delta_l = U_{\parallel}\chi_l + U_{\perp}(\chi_{l+1} + \chi_{l-1})$. Standard self-consistent calculation yields a single-particle gap

$$|\Delta_l| = v_{\text{F}}\alpha_1^{-1}/\sinh[2\pi v_{\text{F}}/(2U_{\perp} - U_{\parallel})] = \Delta_0 \quad (\text{B14})$$

for all chains l that are *not* at a boundary ($l = 1$ or N), and for couplings that satisfy $U_{\perp} > U_{\parallel}/2$. Here, α_1 is the ultraviolet cut-off for the mean-field theory, which is of order α_0 . At temperatures $T > T_{*0} = 4\pi\bar{J}_{\parallel}/k_B$ (or $U_{\parallel} > 0$), we have a null single-particle gap Δ_l at small couplings $U_{\perp} < U_{\parallel}/2$ within mean field. Given the mean-field excitation spectrum $\varepsilon_l^{\pm}(k) = \pm(v_{\text{F}}^2k^2 + |\Delta_l|^2)^{1/2}$ for the fermionic excitations in chain l , the groundstate energy density relative to the decoupled state, $U_{\perp} = 0$, is then equal to

$$[E_{\text{F}}(U_{\perp}) - E_{\text{F}}(0)]/L_x = -\Delta_0^2/4\pi v_{\text{F}}. \quad (\text{B15})$$

By Eq. (B4), the condensation energy per vertical rung is equal to

$$-G_{\text{cond}}^{(0)}/\mathcal{N}' = (a\Delta_0/v_{\text{F}})^2(k_B T/4\pi). \quad (\text{B16})$$

for temperatures $T > T_{*0}$ in the vicinity of the decoupling transition. Eq. (B14) indicates that this quantity vanishes exponentially at the decoupling temperature T_* that is set by the relationship $U_{\parallel} = 2U_{\perp}$.^{42,58}

References

1. G.W. Crabtree and D.R. Nelson, *Physics Today* **50**, 38 (April 1997).
2. E. Zeldov, D. Majer, M. Konczykowski, V.B. Geshkenbein, V.M. Vinokur, and H. Shtrikman, *Nature* **375**, 373 (1995).
3. A. Schilling, R.A. Fisher, N.E. Philips, U. Welp, D. Dasgupta, W.K. Kwok, and G.W. Crabtree, *Nature (London)* **382**, 791 (1996).
4. G. Blatter, M.V. Feigel'man, V.B. Geshkenbein, A.I. Larkin, and V.M. Vinokur, *Rev. Mod. Phys.* **66**, 1125 (1994).
5. B. Khaykovich, M. Konczykowski, E. Zeldov, R.A. Doyle, D. Majer, P.H. Kes, and T.W. Li, *Phys. Rev. B* **56**, R517 (1997).
6. D.T. Fuchs, E. Zeldov, T. Tamegai, S. Ooi, M. Rappaport and H. Shtrikman, *Phys. Rev. Lett.* **80**, 4971 (1998).
7. B. Khaykovich, E. Zeldov, D. Majer, T.W. Li, P.H. Kes, and M. Konczykowski, *Phys. Rev. Lett.* **76**, 2555 (1996).
8. L.I. Glazman and A.E. Koshelev, *Phys. Rev. B* **43**, 2835 (1991).
9. L.L. Daemen, L.N. Bulaevskii, M.P. Maley and J.Y. Coulter, *Phys. Rev. B* **47**, 11291 (1993).
10. A.E. Koshelev, *Phys. Rev. Lett.* **77**, 3901 (1996).
11. A.E. Koshelev, *Phys. Rev. B* **56**, 11201 (1997).
12. M. Feigel'man, V.B. Geshkenbein, and A.I. Larkin, *Physica C* **167**, 177 (1990).
13. E. Frey, D.R. Nelson, and D.S. Fisher, *Phys. Rev. B* **49**, 9723 (1994).
14. T. Chen and S. Teitel, *Phys. Rev. B* **55**, 11766 (1997).
15. X. Hu, S. Miyashita, and M. Tachiki, *Phys. Rev. Lett.* **79**, 3498 (1997); A.K. Nguyen and A. Sudbø, *Phys. Rev. B* **57**, 3123 (1998); P. Olsson and S. Teitel, *Phys. Rev. Lett.* **82**, 2183 (1999).
16. R. Sasik and D. Stroud, *Phys. Rev. Lett.* **75**, 2582 (1995); J. Hu and A.H. MacDonald, *Phys. Rev. B* **56**, 2788 (1997).
17. J.V. José, L.P. Kadanoff, S. Kirkpatrick and D.R. Nelson, *Phys. Rev. B* **16**, 1217 (1977).
18. C. Itzykson and J. Drouffe, *Statistical Field Theory*, vol. 1, (Cambridge Univ. Press, Cambridge, 1991) chap. 4.

19. J.P. Rodriguez, “Nature of Decoupling in the Mixed Phase of Extremely Type-II Layered Superconductors” (cond-mat/9906199).
20. J.P. Rodriguez, *Physica C* **332**, 343 (2000).
21. S.E. Korshunov, *Europhys. Lett.* **11**, 757 (1990).
22. S.E. Korshunov and A.I. Larkin, *Phys. Rev. B* **46**, 6395 (1992).
23. J.P. Rodriguez, *Europhys. Lett.* **31**, 479 (1995).
24. J.P. Rodriguez, *J. Phys. Cond. Matter* **9**, 5117 (1997).
25. J. Friedel, *J. Phys. (Paris)* **49**, 1561 (1988).
26. Z. Tesanovic, *Phys. Rev. B* **59**, 6449 (1999).
27. N. Parga and J.E. Van Himbergen, *Ann. Phys. (N.Y.)* **134**, 286 (1981). [The Coulomb-gas ensemble (12) can be recovered from the “hybrid” one that is derived in this ref. by integrating out the vortex degrees of freedom within layers.]
28. M. Dzierzawa, M. Zamora, D. Baeriswyl and X. Bagnoud, *Phys. Rev. Lett.* **77**, 3897 (1996).
29. S.A. Hattel and J.M. Wheatley, *Phys. Rev. B* **51**, 11951 (1995).
30. M. Franz and S. Teitel, *Phys. Rev. Lett.* **73**, 480 (1994); S. Hattel and J. Wheatley, *Phys. Rev. B* **50**, 16590 (1994); C. E. Creffield and J.P. Rodriguez, unpublished.
31. B.A. Huberman and S. Doniach, *Phys. Rev. Lett.* **43**, 950 (1979); D.S. Fisher, *Phys. Rev. B* **22**, 1190 (1980).
32. D.R. Nelson and B.I. Halperin, *Phys. Rev. B* **19**, 2457 (1979).
33. J.M. Kosterlitz and D.J. Thouless, *J. Phys. C* **6**, 1181 (1973).
34. S. Hikami and T. Tsuneto, *Prog. Theor. Phys.* **63**, 387 (1980); see also S.R. Shenoy and B. Chattopadhyay, *Phys. Rev. B* **51**, 9129 (1995).
35. A.M. Polyakov, *Gauge Fields and Strings* (Harwood, New York, 1987).
36. A.M. Polyakov, *Nucl. Phys. B* **120**, 429 (1977).
37. J.M. Caillol, D. Levesque, J.J. Weis and J.P. Hansen, *J. Stat. Phys.* **28**, 325 (1982); S.W. de Leeuw and J.W. Perram, *Physica (Amsterdam)* **113A**, 546 (1982).
38. A. Polyakov, *Phys. Lett.* **72 B**, 477 (1978).
39. J.P. Rodriguez, *Phys. Rev. B* **51**, 9348 (1995); *Phys. Rev. B* **60**, 3689 (E) (1999).
40. D.R. Nelson and J.M. Kosterlitz, *Phys. Rev. Lett.* **39**, 1201 (1977).
41. J.P. Rodriguez, *Europhys. Lett.* **39**, 195 (1997); *Europhys. Lett.* **47**, 745 (E) (1999).

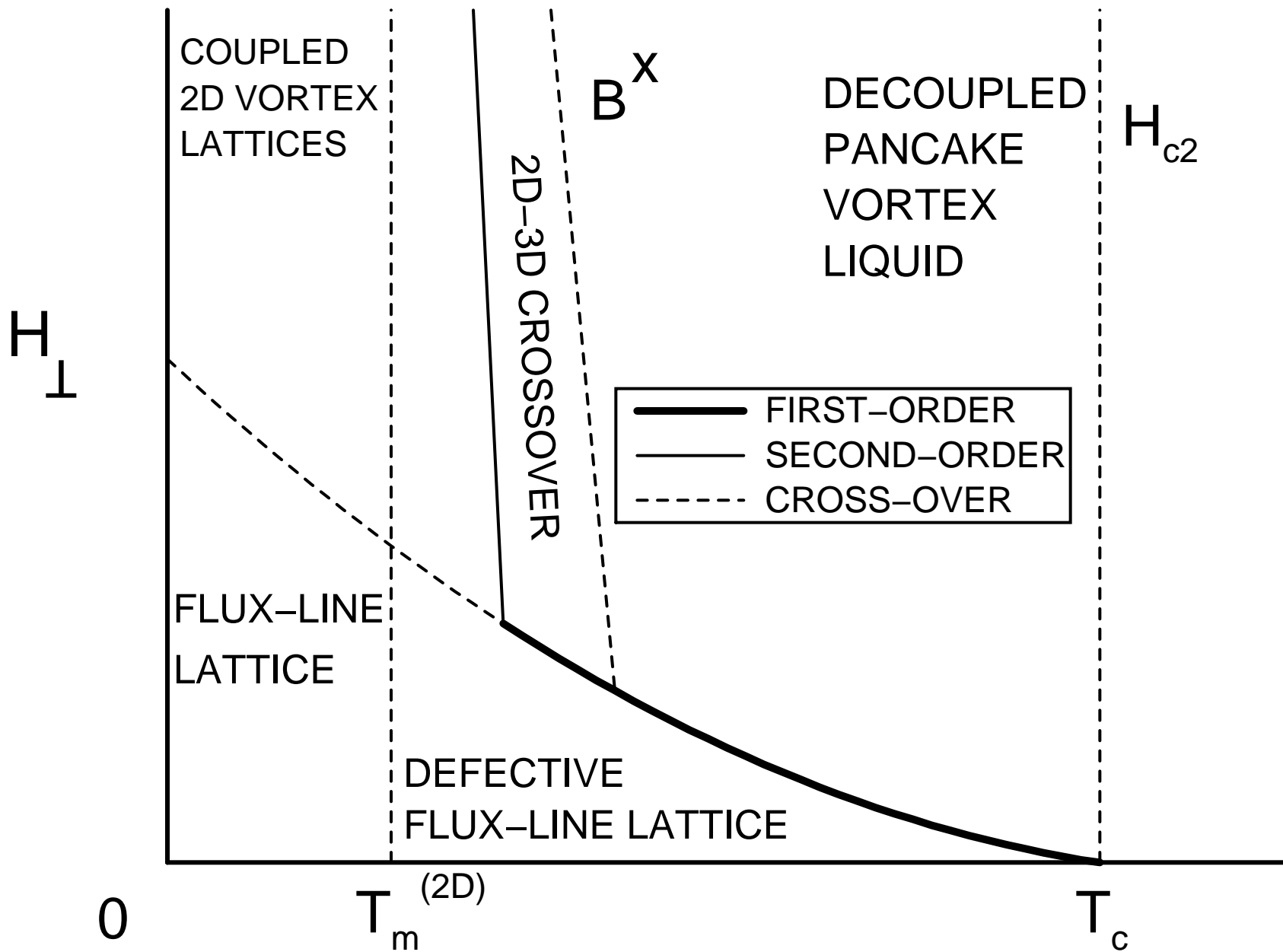
42. J.P. Rodriguez, Phys. Rev. B **58**, 944 (1998).
43. R.F. Dashen, B. Hasslacher, and André Neveu, Phys. Rev. D **11**, 3424 (1975).
44. L.I. Glazman and A.E. Koshelev, Zh. Eksp. Teor. Fiz. **97**, 1371 (1990) [Sov. Phys. JETP **70**, 774 (1990)].
45. V. Ambegaokar and A. Baratoff, Phys. Rev. Lett. **10**, 486 (1963); **11**, 104 (E) (1963).
46. E.B. Sonin, Phys. Rev. Lett. **79**, 3732 (1997).
47. J.M. Kosterlitz, J. Phys. C **7**, 1046 (1974).
48. For a demonstration of a first-order phase transition in the unconfined 2D Coulomb gas, see J. Lee and S. Teitel, Phys. Rev. Lett. **66**, 2100 (1991).
49. G. Blatter, V.B. Geshkenbein and A.I. Larkin, Phys. Rev. Lett. **68**, 875 (1992).
50. A.E. Koshelev, Phys. Rev. Lett. **83**, 187 (1999).
51. Although the Coulomb gas analysis [Eqs. (21) and (60)] indicates a decoupling crossover transition at low temperatures $T < T_m^{(2D)}$ for the case of a finite number of layers, N , the boson analogy used in ref. 13 predicts, on the other hand, a true decoupling/super-solid phase transition in the thermodynamic limit $N \rightarrow \infty$. The compatibility of these two results is assured if the solid to supersolid transition represents a quantum critical point within the boson analogy.
52. D.R. Nelson, in *Phenomenology and Applications of High-Temperature Superconductors*, Proceedings of the Los Alamos Symposium - 1991, edited by K.S. Bedell, M. Inui, D. Meltzer, J.R. Schrieffer and S. Doniach (Addison-Wesley, Reading, MA).
53. J.E. Sonier, J.H. Brewer, R.F. Kiefl, D.A. Bonn, J. Chakhalian, S.R. Dunsiger, W.N. Hardy, R. Liang, W.A. MacFarlane, R.I. Miller, D.R. Noakes, T.M. Riseman and C.E. Stronach, Phys. Rev. B **61**, R890 (2000).
54. G. Blatter, V. Geshkenbein, A. Larkin and H. Nordborg, Phys. Rev. B **54**, 72 (1996).
55. A.E. Koshelev, L.I. Glazman and A.I. Larkin, Phys. Rev. B **53**, 2786 (1996).
56. L.V. Mikheev and E.B. Kolomeisky, Phys. Rev. B **43**, 10431 (1991).
57. B. Horovitz, Phys. Rev. B **47**, 5964 (1993).
58. A. Luther and V.J. Emery, Phys. Rev. Lett. **33**, 589 (1974); S. T. Chui and P. A. Lee, Phys. Rev. Lett. **35**, 315 (1975).

Figure Captions

Fig. 1. Displayed is a schematic phase diagram for a finite number of weakly coupled XY layers with uniform frustration [Eq. (1)]. All artificial pinning effects due to the 2D model grids are suppressed (see refs. 29 and 30). The decoupling (dashed/solid) line is a few to many times the dimensional crossover scale $\Phi_0/\gamma_0'^2 a^2$ at temperatures in the vicinity of $T_m^{(2D)}$ [see Eqs. (60) and (61)]. Also, the Josephson temperature $T_J = J_\perp/k_B$ is assumed to be smaller than the scale of the figure. Last, the solid phase should be defective on scales that are small in comparison to the Josephson penetration length Λ_0 at elevated temperatures $T > T_m^{(2D)}$.

Fig. 2. Shown is a schematic phase diagram for the layered XY model (1) under the assumption that all of the vortex lines are fixed to some type of correlated pin. Vortex/anti-vortex pairs should begin to proliferate at elevated temperatures $T_c^{(2D)} < T < T_c$ inside of the ordered phase on scales that are small in comparison to the Josephson penetration length Λ_0 .

(NO BULK PINNING)



(OPTIMAL PINNING)

